FORMULATION OF A HAAR-WAVELET-BASED MULTI-RESOLUTION ANALYSIS SIMILAR TO THE 3-D FDTD METHOD

Masafumi Fujii and Wolfgang J.R. Hoefer

Department of Electrical and Computer Engineering
University of Victoria
PO BOX 3055, Victoria, B.C. CANADA V8W 3P6
E-mail: fujii@ece.uvic.ca

Abstract—**A 3-D multi-resolution analysis procedure similar to the FDTD method is derived using Haar-wavelets. The method is validated by analyzing several 3-D rectangular resonators with inhomogeneous dielectric loading. It is also applied to the analyses of microstrip low pass filters with open boundaries, and their S-parameters are extracted. The results are compared with those of the traditional FDTD method.**

I. INTRODUCTION

Multi-resolution time-domain (MRTD) techniques using Battle-Lemarie wavelets [1] [2] and Haar wavelets [3] have recently been applied to electromagnetic analysis, and it has been pointed out that these techniques require less computational effort than other time domain techniques.

This paper describes the derivation of an FDTD-like multi-resolution technique based on Haar-wavelets. It is formulated in three-dimensional space and time using 3-D combinations of Haar scaling and wavelet functions at one scaling level, and can handle inhomogeneous dielectric materials. While the accuracy of this new procedure and the memory required are similar to those of the conventional FDTD for the same number of degrees of freedom, it is twice as fast.

To validate the new method, several rectangular cavities with inhomogeneous dielectric loading have been analyzed, and results were compared with analytical results (when available) and data obtained by conventional FDTD analysis having the same number of degrees of freedom, which means that the same amount of computer memory is required in both methods.

Furthermore, the method is applied to the analysis of microstrip low-pass filters with open boundaries, and their S-parameters are extracted. This demonstrates the suitability of the method for solving practical microwave problems. The computer resources required in the proposed method are also discussed and compared with those of the conventional FDTD method.

II. FORMULATION

A. 3-D basis functions and time iterative difference equations

The electric and magnetic field components of Maxwell's curl equations in Cartesian coordinates can be expanded in orthonormal bases of eight three-dimensional combinations of the Haar scaling (ϕ) and wavelet (ψ) functions [4] having the support or the width of the function equal to the spatial discretization interval Δx, Δy and Δz as follows

$$f(x,y,z) = \begin{cases} \phi(x)\,\phi(y)\,\phi(z) \\ \phi(x)\,\phi(y)\,\psi(z) \\ \phi(x)\,\psi(y)\,\phi(z) \\ \psi(x)\,\phi(y)\,\phi(z) \\ \phi(x)\,\psi(y)\,\psi(z) \\ \psi(x)\,\phi(y)\,\psi(z) \\ \psi(x)\,\psi(y)\,\phi(z) \\ \psi(x)\,\psi(y)\,\psi(z) \end{cases} . \tag{1}$$

For example, the expansions of E_x is given by

$$\begin{aligned} E_x(\vec{r},t) = \sum_{i=0}^{I}\sum_{j=0}^{J}\sum_{k=0}^{K}\sum_{n=0}^{N} h_n(t) \\ \cdot\{\, {}^{x}_{n}E^{\phi\phi\phi}_{i+1/2,j,k}\,\phi_{i+1/2}(x)\,\phi_j(y)\,\phi_k(z) \\ +{}^{x}_{n}E^{\phi\phi\psi}_{i+1/2,j,k}\,\phi_{i+1/2}(x)\,\phi_j(y)\,\psi_k(z) \\ +{}^{x}_{n}E^{\phi\psi\phi}_{i+1/2,j,k}\,\phi_{i+1/2}(x)\,\psi_j(y)\,\phi_k(z) \\ +{}^{x}_{n}E^{\psi\phi\phi}_{i+1/2,j,k}\,\psi_{i+1/2}(x)\,\phi_j(y)\,\phi_k(z) \\ +{}^{x}_{n}E^{\phi\psi\psi}_{i+1/2,j,k}\,\phi_{i+1/2}(x)\,\psi_j(y)\,\psi_k(z) \\ +{}^{x}_{n}E^{\psi\phi\psi}_{i+1/2,j,k}\,\psi_{i+1/2}(x)\,\phi_j(y)\,\psi_k(z) \\ +{}^{x}_{n}E^{\psi\psi\phi}_{i+1/2,j,k}\,\psi_{i+1/2}(x)\,\psi_j(y)\,\phi_k(z) \\ +{}^{x}_{n}E^{\psi\psi\psi}_{i+1/2,j,k}\,\psi_{i+1/2}(x)\,\psi_j(y)\,\psi_k(z)\,\} \end{aligned} \tag{2}$$

where the notations are consistent with those used in [5] except that the field value ${}^{x}_{n}E^{\zeta\eta\xi}_{i,j,k}$ with $\zeta,\eta,\xi = \phi,\psi$ denotes

the expansion coefficients in terms of the Haar scaling and wavelet functions at time step n and spatial node i, j, k along the $x-, y-$ and $z-$directions. The function $h_n(t)$ is the unit amplitude rectangular pulse function with the support of $t_n - \Delta t/2 \leq t < t_n + \Delta t/2$ where Δt denotes the time discretization interval.

Similarly, the remaining field components can be expanded in orthonormal basis functions(1). Subsequently, each component is substituted in Maxwell's equations, and the resulting expressions are tested with the product of the spatial basis functions with the pulse function in time, yielding time iterative difference equations. The equations are the same as those appearing in the traditional FDTD method. They are computed for each basis function independently.

B. 3-D boundary conditions

As discussed in [3], the basis functions do not couple at the inner computational nodes, but only at the boundary and excitation nodes. Therefore the electric and magnetic wall conditions are implemented by combining scaling and wavelet functions at the boundaries, so that the tangential electric fields at the boundaries equal to zero. For example, to implement the electric wall condition at $x = 0\,(i = 0)$, the three-dimensional Haar basis functions are divided into four pairs as follows:

$$\begin{aligned}&\big(g(x,y,z), h(x,y,z)\big)\\ &\quad= \begin{cases} \big(\phi(x)\,\phi(y)\,\phi(z),\ \psi(x)\,\phi(y)\,\phi(z)\big)\\ \big(\phi(x)\,\phi(y)\,\psi(z),\ \psi(x)\,\phi(y)\,\psi(z)\big)\\ \big(\phi(x)\,\psi(y)\,\phi(z),\ \psi(x)\,\psi(y)\,\phi(z)\big)\\ \big(\phi(x)\,\psi(y)\,\psi(z),\ \psi(x)\,\psi(y)\,\psi(z)\big)\end{cases}. \end{aligned} \tag{3}$$

Then, at every time step n the tangential electric fields E_y and E_z at the boundary are set to zero by selecting the coefficients of the pair basis functions (3) as

$$ {}^{\xi}_{n}E^{g}_{0jk} = -{}^{\xi}_{n}E^{h}_{0jk} = \frac{1}{4}({}^{\xi}_{n}E^{g}_{1jk} + {}^{\xi}_{n}E^{h}_{1jk})\,,\ \xi = y, z\,. \tag{4}$$

At $x = x_{max}\,(i = i_{max})$, with the same pairs, the coefficients of the basis functions are given by

$$\begin{aligned} {}^{\xi}_{n}E^{g}_{i_{max}jk} = {}^{\xi}_{n}E^{h}_{i_{max}jk} \quad &= \quad \frac{1}{4}({}^{\xi}_{n}E^{g}_{i_{max}-1\,jk} - {}^{\xi}_{n}E^{h}_{i_{max}-1\,jk})\,,\\ &\quad \xi = y, z\,. \end{aligned} \tag{5}$$

Similarly, the boundary conditions at $y = 0, y_{max}$ and $z = 0, z_{max}$ can be derived. Equations (4) and (5) are computed for the coefficients of all basis functions.

C. Sampling of the field value

In this proposed method, the space is discretized by using the conventional Yee cell. However, each field node is divided into eight sub-nodes as shown in Fig. 1. The sub-nodes are named lll, llu, lul, and so on, corresponding to the *l*ower or *u*pper position with respect to the original field node along the x-, y- and z-axes. The field values at the sub-nodes E^{opq} with $o, p, q = l, u$ can be calculated from the three-dimensional Haar basis coefficients $E^{\zeta\eta\xi}$ with $\zeta, \eta, \xi = \phi, \psi$ as

$$\begin{pmatrix} E^{lll}\\ E^{llu}\\ E^{lul}\\ E^{ull}\\ E^{luu}\\ E^{ulu}\\ E^{uul}\\ E^{uuu}\end{pmatrix} = A \begin{pmatrix} E^{\phi\phi\phi}\\ E^{\phi\phi\psi}\\ E^{\phi\psi\phi}\\ E^{\psi\phi\phi}\\ E^{\phi\psi\psi}\\ E^{\psi\phi\psi}\\ E^{\psi\psi\phi}\\ E^{\psi\psi\psi}\end{pmatrix}, \tag{6}$$

with the basis transformation matrix

$$A = \frac{1}{\sqrt{8}} \begin{pmatrix} +1 & +1 & +1 & +1 & +1 & +1 & +1 & +1\\ +1 & -1 & +1 & +1 & -1 & -1 & +1 & -1\\ +1 & +1 & -1 & +1 & -1 & +1 & -1 & -1\\ +1 & +1 & +1 & -1 & +1 & -1 & -1 & -1\\ +1 & -1 & -1 & +1 & +1 & -1 & -1 & +1\\ +1 & -1 & +1 & -1 & -1 & +1 & -1 & +1\\ +1 & +1 & -1 & -1 & -1 & -1 & +1 & +1\\ +1 & -1 & -1 & -1 & +1 & +1 & +1 & -1\end{pmatrix}. \tag{7}$$

Matrix A has an orthogonality property $A^{-1} = A^{\dagger}$, where $A^{\dagger}$ denotes the transpose matrix of A. Furthermore, it is symmetric $A^{\dagger} = A$. Therefore, it has the important property

$$A^{-1} = A\,, \tag{8}$$

which allows an simple conversion between the field values at the sub-nodes and the Haar basis coefficients.

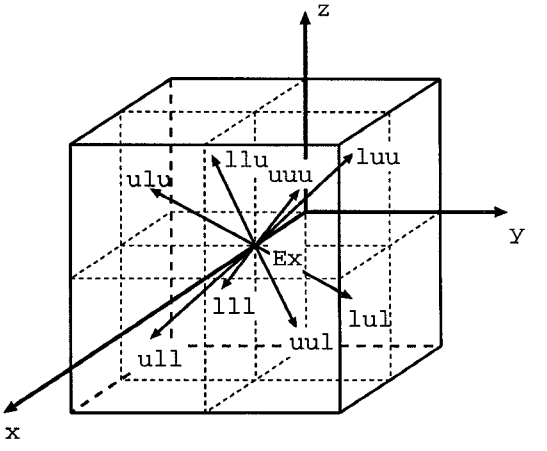

Fig. 1. Eight sub-E_x-nodes form a standard FDTD node of E_x

D. Perfect electric conductor conditions

For the perfect electric conductor condition, the tangential electric field along the conductor is set to zero by canceling the fields associated with the scaling and the wavelet functions the axis of which is perpendicular to the conductor surface. In the case of a conductor lying on the xy-plane and located at the sub-nodes E^{lll}_{ijk}, E^{lul}_{ijk}, E^{ull}_{ijk} and E^{uul}_{ijk}, the field values at the rest of the sub-nodes E^{llu}_{ijk}, E^{luu}_{ijk}, E^{ulu}_{ijk} and E^{uuu}_{ijk} are determined by the average between upper and lower sides of the sub-nodes. The sub-nodes on one side are zero since they are lying on the conductor surface, thus,

$$\begin{pmatrix} {}^{\omega}E^{lll}_{ijk} \\ {}^{\omega}E^{llu}_{ijk} \\ {}^{\omega}E^{lul}_{ijk} \\ {}^{\omega}E^{ull}_{ijk} \\ {}^{\omega}E^{luu}_{ijk} \\ {}^{\omega}E^{ulu}_{ijk} \\ {}^{\omega}E^{uul}_{ijk} \\ {}^{\omega}E^{uuu}_{ijk} \end{pmatrix} = \frac{1}{2} \begin{pmatrix} 0 \\ {}^{\omega}E^{lll}_{ijk+1} \\ 0 \\ 0 \\ {}^{\omega}E^{lul}_{ijk+1} \\ {}^{\omega}E^{ull}_{ijk+1} \\ 0 \\ {}^{\omega}E^{uul}_{ijk+1} \end{pmatrix}, \text{with } \omega = x, y. \quad (9)$$

Hence, the expansion coefficients for the three-dimensional basis functions for E_x and E_y components can be calculated as

$$\begin{pmatrix} {}^{\omega}E^{\phi\phi\phi}_{ijk} \\ {}^{\omega}E^{\phi\phi\psi}_{ijk} \\ {}^{\omega}E^{\phi\psi\phi}_{ijk} \\ {}^{\omega}E^{\psi\phi\phi}_{ijk} \\ {}^{\omega}E^{\phi\psi\psi}_{ijk} \\ {}^{\omega}E^{\psi\phi\psi}_{ijk} \\ {}^{\omega}E^{\psi\psi\phi}_{ijk} \\ {}^{\omega}E^{\psi\psi\psi}_{ijk} \end{pmatrix} = A \begin{pmatrix} {}^{\omega}E^{lll}_{ijk} \\ {}^{\omega}E^{llu}_{ijk} \\ {}^{\omega}E^{lul}_{ijk} \\ {}^{\omega}E^{ull}_{ijk} \\ {}^{\omega}E^{luu}_{ijk} \\ {}^{\omega}E^{ulu}_{ijk} \\ {}^{\omega}E^{uul}_{ijk} \\ {}^{\omega}E^{uuu}_{ijk} \end{pmatrix} = \frac{1}{2} A \begin{pmatrix} 0 \\ {}^{\omega}E^{lll}_{ijk+1} \\ 0 \\ 0 \\ {}^{\omega}E^{lul}_{ijk+1} \\ {}^{\omega}E^{ull}_{ijk+1} \\ 0 \\ {}^{\omega}E^{uul}_{ijk+1} \end{pmatrix},$$

$$\text{with } \omega = x, y. \quad (10)$$

E. Absorbing boundary conditions

Mur's first order absorbing boundary condition (ABC) has been implemented. The ABCs in the traditional FDTD method can be implemented independently for each coefficient associated with the three-dimensional Haar basis function. The outgoing wave associated with each basis function is absorbed independently by each associated ABC. Therefore, the implementation in the new scheme is the same as that in the traditional FDTD method.

III. Validation and Comparison with FDTD

Four rectangular cavities loaded with inhomogeneous dielectric materials [6] were analyzed with the new multi-resolution method. The dominant resonant frequencies were compared with analytical values (when available) and those obtained with the conventional FDTD method. The geometries of the four cavities are shown in Fig. 2 and the results are summarized in Table I.

The time discretization interval was chosen to be 0.8 times the Courant limit for both methods. Because the time discretization interval is twice that of the traditional FDTD method, the computational time is approximately half that of the traditional FDTD method for the same number of degrees of freedom.

The number of cells in the multi-resolution scheme is approximately one eighth of the number of FDTD cells so that the number of degrees of freedom is the same for both methods. To discretize the geometry of the dielectric materials accurately, nonuniform grids were incorporated in the cases (b),(c) and (d). In the case of the homogeneous dielectric cavity (a), the results obtained with both methods agreed within ±1%.

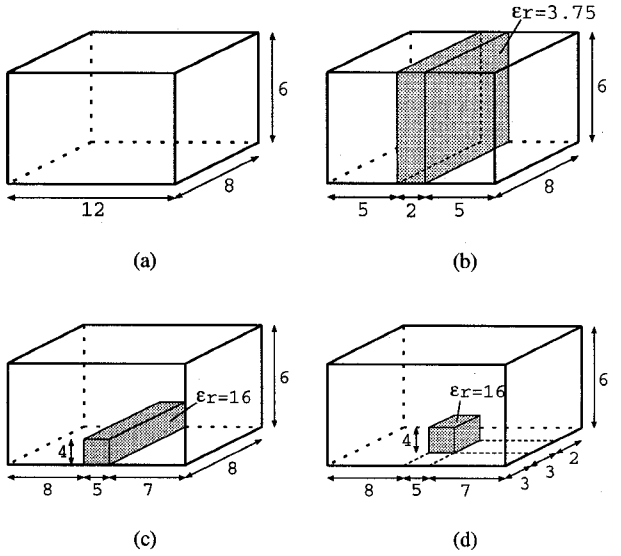

Fig. 2. Three-dimensional rectangular cavities analyzed in this study

IV. Analysis of Microstrip Low Pass Filters

The proposed method was applied to the analysis of the microstrip low pass filter shown in Fig. 3 [7]. The Yee grid lines used in the analysis are shown in the figure together with the geometrical dimensions. To accurately discretize the geometry of the circuit, nonuniform grids were incorporated.

The structure was also analyzed with the conventional FDTD method under the condition described in [7]. The analysis conditions for the proposed method are listed in Table II together with those of the conventional FDTD method.

The discretization was such that the number of degrees

TABLE I

NORMALIZED DOMINANT RESONANT FREQUENCIES OF RECTANGULAR CAVITIES

cavity	new scheme (i) (Yee cells)	conventional FDTD (ii) (Yee cells)	% difference $\frac{(i)-(ii)}{(ii)}$	analytical
(a)	0.07542 (6x4x3)	0.07486 (12x8x6)	+0.75	0.07511
(b)	0.05302 (5x4x3)	0.05228 (12x8x6)	+1.42	0.05221
(c)	0.02764 (10x4x3)	0.02661 (20x8x6)	+3.87	—
(d)	0.03834 (10x5x3)	0.03908 (20x8x6)	–1.89	—

of freedom was the same for both methods. The calculation time for the proposed method was about half that of the conventional FDTD method. This was due to the time discretization interval being approximately twice that of the conventional FDTD method, which was achieved by making the minimum grid dimension approximately twice that of the conventional FDTD method having the same number of degrees of freedom.

TABLE II

ANALYSIS CONDITIONS FOR THE MICROSTRIP LOW PASS FILTER

	new scheme	conventional FDTD
Yee cells	49x39x8 (non-uniform)	100x80x16 (uniform)
computational time	11m 32.5s	20m 45.5s
time steps	2560	4000

The resulting S-parameters (S_{11}, S_{21}) are shown in Fig. 4. The results indicate good agreement between both methods, except for slight deviations in the high frequency range over 16GHz and in the small signal range below –30dB.

V. CONCLUSIONS

A 3-D multi-resolution analysis procedure similar to the FDTD method has been derived by using three-dimensional Haar scaling and wavelet functions.

The resulting method has been tested and validated by analyzing four inhomogeneously filled rectangular cavities. The method has also been applied to the analysis of microstrip low pass filters. The resulting S-parameters are in good agreement with those obtained with the conventional FDTD method. The calculation time for the proposed method was approximately half that of the equivalent conventional FDTD method.

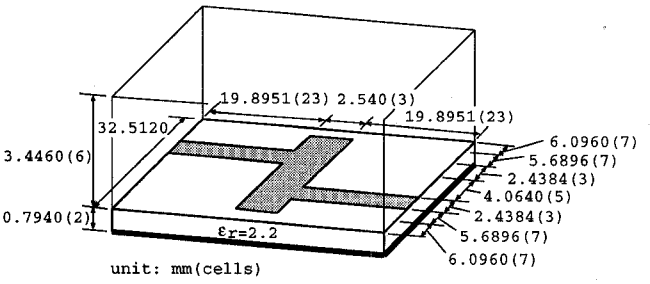

Fig. 3. Microstrip low pass filter configuration under investigation

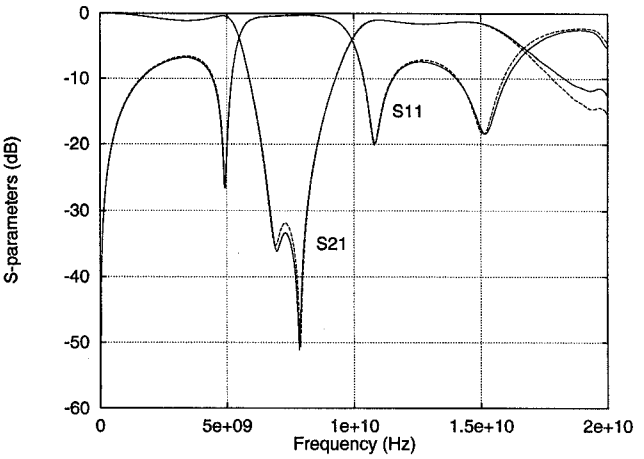

Fig. 4. Computed S-parameters (S_{11}, S_{21}) of the filter, — : proposed method, - - - : conventional FDTD method

REFERENCES

[1] M.Krumpholz and L.P.B.Katehi, "New prospects for time domain analysis", *IEEE Microwave Guided Wave Lett.*, vol. 5, no. 11, pp. 382–384, 1995.

[2] E.Tentzeris, R.Robertson, L.P.B.Katehi, and A.Cangellaris, "Space- and time-adaptive gridding using MRTD technique", *1997 IEEE MTT-S International Microwave Symposium Digest*, pp. 337–340.

[3] K.Goverdhanam, L.P.B.Katehi, and A.Cangellaris, "Application of multiresolution based FDTD multigrid", *1997 IEEE MTT-S International Microwave Symposium Digest*, pp. 333–336.

[4] I.Daubechies, *Ten lectures on wavelets*, SIAM Rev, Philadelphia, PA, 1992.

[5] M.Krumpholz and L.P.B.Katehi, "MRTD: New time-domain schemes based on multiresolution analysis", *IEEE Trans. Microwave Theory Tech.*, vol. 44, no. 4, pp. 555–571, 1996.

[6] D.H.Choi and W.J.R.Hoefer, "The finite-difference–time-domain method and its application to eigenvalue problems", *IEEE Trans. Microwave Theory Tech.*, vol. 34, no. 12, pp. 1464–1470, 1986.

[7] D.M.Sheen, S.M.Ali, M.D.Abouzahra, and J.A.Kong, "Application of the three-dimensional finite-difference time-domain mathod to the analysis of planar microstrip circuits", *IEEE Trans. Microwave Theory Tech.*, vol. 38, no. 7, pp. 849–857, 1990.